UCRL-PROC-215254

LAWRENCE
LIVERMORE
NATIONAL
LABORATORY

Z-Beamlet (ZBL) Multi-Frame Back-lighter (MFB) System for ICF/Plasma Diagnostics

J.A. Caird, A.C. Erlandson, W.A. Molander, J.E. Murray, G.K. Robertson, I.C. Smith, D.B. Sinars, J.L. Porter

September 10, 2005

Fourth International Conference on Inertial Fusion Sciences and Applications (IFSA2005)
Biarritz, France
September 4, 2005 through September 9, 2005

WPo16.4
Z-Beamlet (ZBL) Multi-Frame Back-lighter (MFB) System for ICF/Plasma Diagnostics

J. A. Caird, A. C. Erlandson, W. A. Molander, and J. E. Murray
Lawrence Livermore National Laboratory, 7000 East Ave., L-470, Livermore, CA 94550-9234 USA
Phone: (925) 422-6159, FAX: (925) 423-6195, email: caird@llnl.gov

G. K. Robertson, I. C. Smith, D. B. Sinars, and J. L. Porter
Sandia National Laboratories, P.O. Box 5800, Mail Stop 1193
Albuquerque, NM 87185-1193 USA

Abstract

Z-Beamlet [1] is a single-beam high-energy Nd:glass laser used for backlighting high energy density (HED) plasma physics experiments at Sandia's Z-accelerator facility. The system currently generates a single backlit image per experiment, and has been employed on approximately 50% of Z-accelerator system shots in recent years. We have designed and are currently building a system that uses Z-Beamlet to generate two distinct backlit images with adjustable time delay ranging from 2 to 20 ns between frames. The new system will double the rate of data collection and allow the temporal evolution of high energy density phenomena to be recorded on a single shot.

1. INTRODUCTION

The Z facility at Sandia National Laboratories in New Mexico is the pulsed-power driver for a z-pinch plasma radiation source, which produces 20 MA peak current with 100 ns rise-time [2]. The current from the driver passes through a cylindrical array of wires that vaporize and form plasma. The $J \times B$ force compresses the plasma to the axis of the system to generate more than 200 TW and 1-2 MJ of x-ray radiation to drive high energy density physics experiments. X-ray backlighting is the primary diagnostic for many of these experiments because of the large-scale, dense plasmas involved.

The Z-Beamlet Laser (ZBL) is a multi-kilojoule, terawatt-class Nd:glass laser that can be focused to a peak intensity of over 10^{16} W/cm^2 at the frequency doubled wavelength of 527-nm [1]. This class of laser is able to generate bright x-ray sources in the 1-10 keV x-ray spectral range that are ideally suited for x-ray radiography of a wide variety of high-energy-density experiments conducted at the Z-facility [3]. Many of the components of Z-Beamlet were originally developed and tested as part of the Beamlet laser at Lawrence Livermore National Laboratory where it was built as a scientific prototype for the National Ignition Facility [4]. The laser is housed in a separate 900-m^2 building with a telescope to transport its beam to the adjacent Z-facility as shown in Figure 1.

To date, the ZBL has been used to generate only a single x-ray radiograph for each high-energy-density

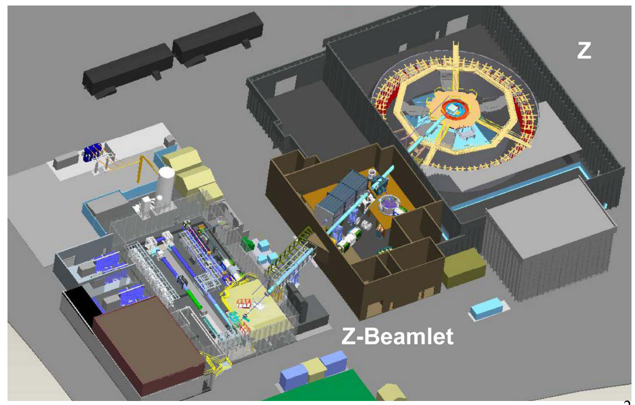

Figure 1. A telescope transports laser pulses from the 900-m^2 ZBL building to the adjacent Z-facility.

physics experiment performed at the Z-facility. The object of the present development project is to enable multiple x-ray radiographs to be taken sequentially during each Z-shot.

The initial demonstration of multi-frame backlighting on Z will use a detection system based on bent crystal x-ray imaging [5]. This system uses the Bragg condition to reflect monochromatic x-rays at well defined angles, and spherical optics to form x-ray images of the laser point source, as well as the object(s) to be radiographed, as shown in Figure 2.

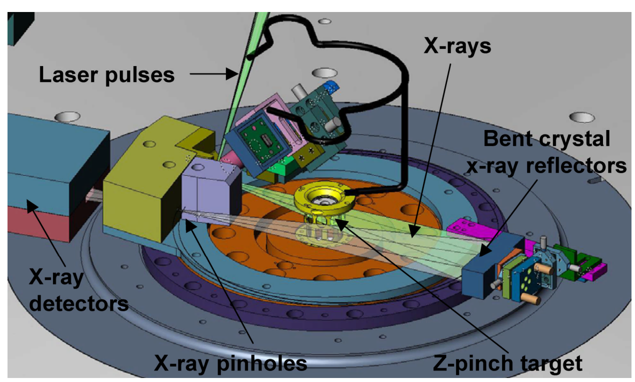

Figure 2. Bent crystal x-ray imaging system in Z target chamber.

2. ARCHITECTURE

To add Multi-Frame Backlighting capability the output of ZBL's front end will be split, with roughly half of its output delayed using a variable length optical trombone as shown in Figure 3. The pulses are then recombined with a small angular separation (i.e., angle multiplexed) and amplified in the main Z-Beamlet 4-pass disk amplifier cavity. One of the beams is also de-collimated slightly using a positive-negative lens-pair in the trombone so that the two beams ultimately focus in the target chamber at locations that are both laterally and longitudinally separated. In the baseline design the two focal spots in the target chamber are separated by 4.3-mm laterally and 10-mm longitudinally, as shown in Figure 4. X-rays generated in metal targets located at the laser focal spots pass through the Z-pinch target and are imaged independently by two bent-crystal imaging systems [5] such that the two x-ray images are spatially separated for recording.

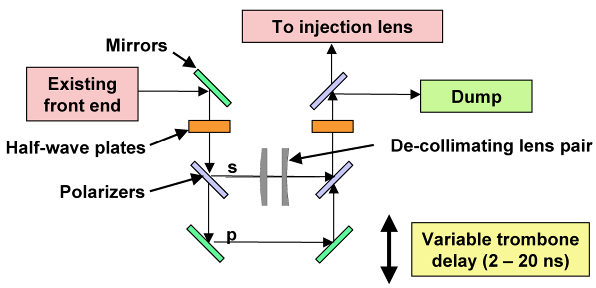

Figure 3. Half-wave plates and polarizers control energy split between the two pulses. The half-wave plates can be oriented to provide nearly 100% transmission in either path for alignment.

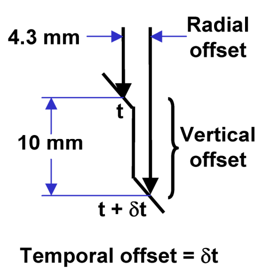

Figure 4. Target chamber focal spots in the will be separated in space as well as time due to angle multiplexing. De-collimation of one beam produces vertical offset at the "stepped target."

The normal configuration of Z-Beamlet's main disk amplifier cavity is depicted schematically in Figure 5. A pulse from the front end is injected through pinhole #1, expands as it propagates to cavity spatial filter lens L_1 where it is collimated before double-passing the main cavity disk amplifiers. After the second pass the beam is focused through pinhole #2, expands to lens L_2 where it is again collimated for propagation to the Plasma Electrode Pockel's Cell (PEPC). The PEPC is turned on prior to the arrival of the pulse so that its polarization can be rotated 90 degrees allowing it to transmit through the polarizer, and be reflected by M_2. The pulse then transmits through the polarizer again and the PEPC rotates its polarization back to the original orientation for amplification in passes 3 and 4 through the main cavity disk amplifiers. After the 4th pass through the amplifiers the PEPC is turned off, the polarization is not rotated, and the pulse is reflected out of the cavity, on to the frequency converter, and then into the Z target chamber final focus system.

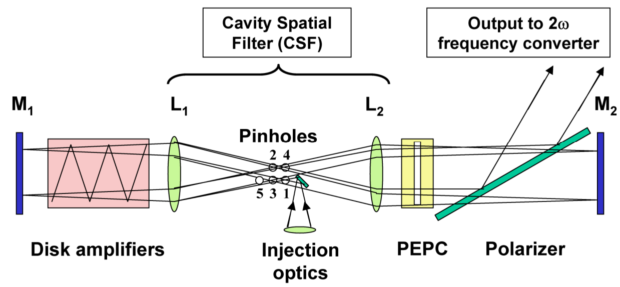

Figure 5. Standard configuration of ZBL's main disk amplifier cavity.

An end view depicting alignment of rays through ZBL's main amplifier cavity is shown on the left side of Figure 6. M_1 is oriented so that rays coming from pinhole #1 are imaged to pinhole #2. M_2 is oriented so that rays from pinhole #2 are imaged to pinhole #3. Rays from pinhole #3 are reflected to output pinhole #4 by M_1, and any depolarized light not coupled out of the cavity on pass 4 reflects from M_2 and is focused into a beam dump located near virtual pinhole #5.

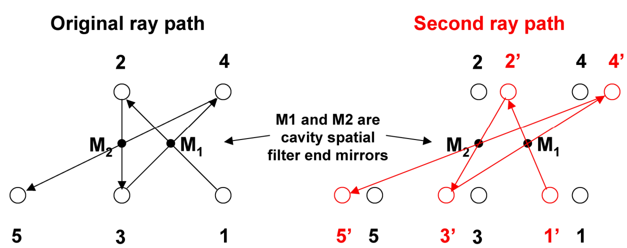

Figure 6. End view of ray paths through the main cavity amplifiers and spatial filter pinholes.

The ray path for a second pulse will be established by orienting the polarizers of Figure 3 so that the injected pulse is focused to pinhole 1' (right side of Figure 6). The alignment of mirrors M1 and M2 established for the first beam then naturally relay the beam through pinholes 2', 3' and 4' as depicted. The same distance separates output pinholes 4 and 4' as input pinholes 1 and 1'. Depolarized light is sent to a beam dump at virtual pinholes 5 and 5'. New beam injection and pinhole manipulation hardware has been designed for the cavity spatial filter as shown in Figure 7.

The main advantage of angle multiplexing is that it allows virtually all of Z-Beamlet's 35-cm clear-aperture to amplify both pulses so that each pulse can have the full B-integral-limited output energy. Furthermore, our analysis shows that both the angular separation and the de-collimation are small enough that the main cavity's KDP optical switch and the output's Type-I KDP frequency converter operation are negligibly affected.

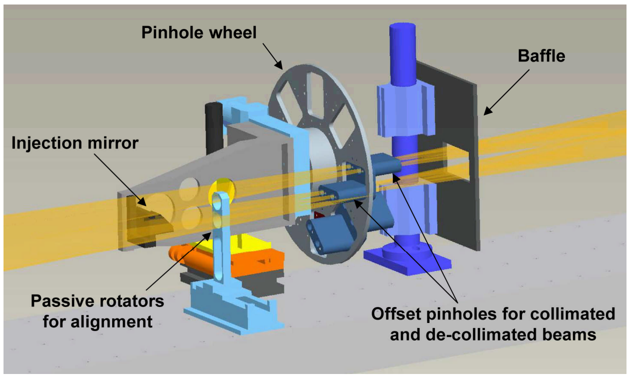

Figure 7. New CSF pinhole manipulation hardware for the Z-Beamlet Laser's Multi-Frame Backlighter.

3. PENCIL BEAMS

Ghost reflections from spatial filter lenses pass through the pinholes to form pencil beams propagating backward through the laser system. The pencil beams can cause problems if not properly managed. Doubling the number of pinholes in the cavity spatial filter doubles the number of pencil beams that are generated (per output pulse). Moreover, doubling the number of output pulses in addition to doubling the number of pinholes will increase the number of pencil beams by a factor of 4. To mitigate the risk of additional pencil beams we studied their propagation in detail.

Ghost reflections from L_2 come to a focus before passing through the CSF pinholes. At any point optically conjugate to this focus, the pencil beams overlap. Following passage through the pinholes they are focused by L_1, and amplified by the main cavity amplifiers. The set originating at the output surface of L_2 come to focus and overlap near the last slab, C_{11}, of the main cavity amplifier. Interference of the overlapping pencil beams increases the peak intensity in the vicinity of C_{11} by an order of magnitude. The calculated interference pattern is shown in Figure 8 for the original ZBL operation. If the anti-reflection coating on the second surface of L_2 is allowed to increase to 1% then predicted fluence at C_{11} (13 J/cm^2) is still below the damage threshold of the optic. A horizontal lineout from the pattern in Figure 8 is shown in Figure 9. These results assume complete overlap of all the pencil beams. Due to optical aberrations, the pencil beams do not perfectly overlap so the enhancement will not be quite as large as indicated here.

For ZBL-MFB the number of pencil beams doubles, and the peak fluence at the point of overlap near C_{11} increases by a factor of 4 as shown in Figures 10 and 11. The peak fluence is now 52 J/cm^2 for 1% reflectivity of L_2, and well above the expected damage threshold.

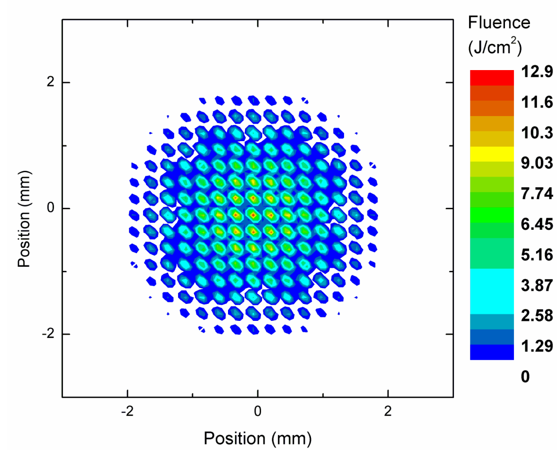

Figure 8. Interference pattern at pencil beam overlap near amplifier slab C_{11} for normal ZBL operation with 1% reflectivity at output surface of L_2.

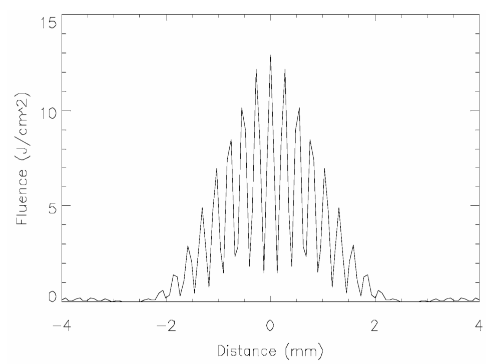

Figure 9. Horizontal lineout through pattern of Figure 8.

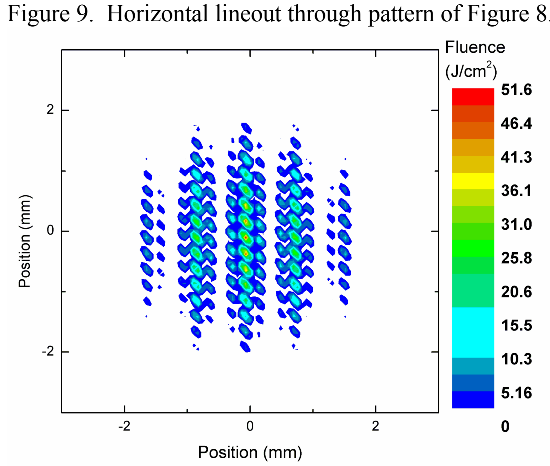

Figure 10. Interference pattern at pencil beam overlap near amplifier slab C_{11} for ZBL-MFB operation with 1% reflectivity at output surface of L_2.

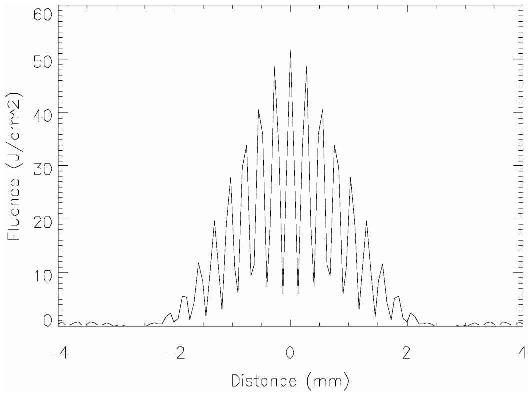

Figure 11. Vertical lineout through pattern of Figure 10.

There are a number of ways to reduce the damage risk associated with the increased number of pencil beams. The first is to ensure that L_2's anti-reflection coating remains good (less than 0.2% reflectivity is recommended). A second way is to decrease the size of the spatial filter pinholes. Since the throughput of the pinholes scales as the square of their size, and the diffraction limited spot size at the point of pencil beam overlap scales inversely with the pinhole size, the peak fluence at that location scales as the 4th power of the pinhole size. Reducing the spatial filter pinhole size, therefore, dramatically reduces the damage threat. Other potential methods of mitigation include tilting L_2, or refiguring the lens surfaces to place the ghost foci in more benign locations.

4. CONCLUSION

The ZBL-MFB upgrade will enable collection of two independent x-ray images of high energy density physics experiments at Z with variable time delay of 2 to 20 ns. This will enable direct measurement of the temporal evolution of events for the first time. Angle multiplexing of the beams will be used so that both pulses can have full aperture, and full output energy. Frequency conversion and Pockel's cell operation will not be significantly affected. Laser diagnostics will be upgraded to allow full characterization of both pulses. Reducing spatial filter pinhole size will mitigate the increase in fluence at the location of pencil beam overlap. Experiments are scheduled to demonstrate the MFB capability in an offline target chamber near the end of 2005, with operation in the Z target chamber scheduled for 2006.

Acknowledgement

This work was performed under the auspices of the U.S. Department of Energy by the University of California Lawrence Livermore National Laboratory under contract No. W-7405-Eng-48.

REFERENCES

[1] P.K. Rambo, I.C. Smith, J.L. Porter Jr., M.J. Hurst, C.S. Spease, R.G. Adams, A.J. Garcia, E. Dawson, B.D. Thurston, C. Wakefield, J.W. Kellogg, M.J. Slattery, H.C. Ives III, R.S. Broyles, J.A. Caird, A.C. Erlandson, J.E. Murray, W.C. Behrendt, N.D. Nielsen, and J.M. Narduzzi, "Z-Beamlet: A multikilojoule, terawatt-class laser system," Appl. Opt. **44**, 2421-2430 (2005).

[2] R.B. Spielman, C. Deeney, G.A. Chandler, M.R. Douglas, D.L. Fehl, M.K.Matzen, D.H. McDaniel, T.J. Nash, J.L. Porter, T.W.L. Sanford, J.F. Seaman, W.A. Stygar, K.W. Struve, S.P. Breeze, J.S. McGurn, J.A. Torres, D.M. Zagar, T.L. Gilliland, D.O. Jobe, J.L. McKinney, R.C. Mock, M. Vargas, and T. Wagoner, "Tungsten wire-array Z-pinch experiments at 200 TW and 2 MJ," Phys. Plasmas **5**, 2105-2111 (1998).

[3] G.R. Bennett, O.L. Landen, R.G. Adams, J.L. Porter, L.E. Ruggles, W.W. Simpson, and C. Wakefield, "X-ray imaging techniques on Z using the Z-Beamlet laser," Rev. Sci. Instrum. **72**, 657-662 (2001).

[4] B.M. Van Wonterghem, J.R. Murray, J.H. Campbell, D.R. Speck, C.E. Barker, I.C. Smith, D.F. Browning, and W.C. Behrendt, "Performance of a prototype for a large-aperture multipass Nd:glass laser for inertial confinement fusion, "Appl. Opt. **36**, 4932-4953 (1997).

[5] D.B. Sinars, G.R. Bennett, D.F. Wenger, M.E. Cuneo, D.L. Hanson, J.L. Porter, R.G. Adams, P.K. Rambo, D.C. Rovang, and I.C. Smith, "Monochromatic x-ray imaging experiments on the Sandia National Laboratory's Z facility," *Rev. Sci. Instr.* **75**, 3672-3677, (2004).